

Fluctuation dynamo and turbulent induction at low magnetic Prandtl numbers

A A Schekochihin,^{1,2,3} A B Iskakov,⁴ S C Cowley,^{1,4}
J C McWilliams,⁵ M R E Proctor,³ T A Yousef³

¹ Blackett Laboratory, Imperial College, London SW7 2BW, UK

² King's College, Cambridge CB2 1ST, UK

³ DAMTP, University of Cambridge, Cambridge CB3 0WA, UK

⁴ Department of Physics and Astronomy, UCLA, Los Angeles, CA 90095-1547, USA

⁵ Department of Atmospheric Sciences, UCLA, Los Angeles, CA 90095-1565, USA

E-mail: a.schekochihin@imperial.ac.uk

Abstract. This paper is a detailed report on a programme of direct numerical simulations of incompressible nonhelical randomly forced MHD turbulence that are used to settle a long-standing issue in the turbulent dynamo theory and demonstrate that the fluctuation dynamo exists in the limit of large magnetic Reynolds number $Rm \gg 1$ and small magnetic Prandtl number $Pm \ll 1$. The dependence of the critical Rm_c for dynamo vs. the hydrodynamic Reynolds number Re is obtained for $1 \lesssim Re \lesssim 6700$. In the limit $Pm \ll 1$, Rm_c is at most three times larger than for the previously well established dynamo at large and moderate Prandtl numbers: $Rm_c \lesssim 200$ for $Re \gtrsim 6000$ compared to $Rm_c \sim 60$ for $Pm \geq 1$. The stability curve $Rm_c(Re)$ (and, it is argued, the nature of the dynamo) is substantially different from the case of the simulations and liquid-metal experiments with a mean flow. It is not as yet possible to determine numerically whether the growth rate of the magnetic energy is $\propto Rm^{1/2}$ in the limit $Re \gg Rm \gg 1$, as should be the case if the dynamo is driven by the inertial-range motions at the resistive scale, or tends to an Rm -independent value comparable to the turnover rate of the outer-scale motions. The magnetic-energy spectrum in the low- Pm regime is qualitatively different from the $Pm \geq 1$ case and appears to develop a negative spectral slope, although current resolutions are insufficient to determine its asymptotic form. At $Rm \in (1, Rm_c)$, the magnetic fluctuations induced via the tangling by turbulence of a weak mean field are investigated and the possibility of a k^{-1} spectrum above the resistive scale is examined. At low $Rm < 1$, the induced fluctuations are well described by the quasistatic approximation; the $k^{-11/3}$ spectrum is confirmed for the first time in direct numerical simulations. Applications of the results on turbulent induction to understanding the nonlocal energy transfer from the dynamo-generated magnetic field to smaller-scale magnetic fluctuations are discussed. The results reported here are of fundamental importance for understanding the genesis of small-scale magnetic field in cosmic plasmas.

PACS numbers: 91.25.Cw, 47.65.-d, 95.30.Qd, 96.60.Hv, 47.27.ek

1. Introduction

The dynamo effect, or amplification of magnetic field by fluid motion is a fundamental physical mechanism most likely to be responsible for the ubiquitous presence of dynamically strong magnetic fields in the Universe — from planets and stars to galaxies and galaxy clusters (e.g., Moffatt 1978, Childress & Gilbert 1995, Roberts & Glatzmaier 2000, Ossendrijver 2003, Widrow 2002). It is important to distinguish between two main types of dynamo. The first is the large-scale, or *mean-field dynamo* defined as the growth of magnetic field at scales larger than the scale of the fluid motion. If the fluid is turbulent, this refers to the outer (energy-containing) scale, denoted here by L . In this paper, we shall not be concerned with this type of dynamo and concentrate on the second kind, the small-scale, or *fluctuation dynamo*, which is defined as the growth of magnetic-fluctuation energy at or below the outer scale of the motion. Note that if a large-scale magnetic field, dynamo-generated or otherwise, is present, there will always be some tangling of this field by the fluid, giving rise to small-scale magnetic fluctuations. This effect, known as the *magnetic induction*, should not be confused with the fluctuation dynamo, although it can often be difficult to tell which of the two is primarily responsible for the presence of magnetic energy at small scales.

Despite its very generic nature, the presence of dynamo action in any particular system is usually impossible to prove analytically. This is especially true in the astrophysically relevant limit of large hydrodynamic and magnetic Reynolds numbers, $Re \gg 1$ and $Rm \gg 1$, when the fluid motion is turbulent. Numerical experiments have, therefore, played a crucial role in building up the case for the turbulent dynamo (e.g., Galloway & Proctor 1992, Meneguzzi et al. 1981, Cattaneo 1999, Brandenburg 2001). These have recently been joined by a successful laboratory demonstration of the dynamo action in a geometrically unconstrained turbulence of liquid sodium (Monchaux et al. 2007, Berhanu et al. 2007). However, both in the laboratory and in the computer, it has proven very hard to access the parameter regimes that are sufficiently asymptotic in both Re and Rm to resemble real astrophysical situations.

The key parameter that makes the situation difficult is the magnetic Prandtl number, $Pm = Rm/Re = \nu/\eta$ (viscosity/magnetic diffusivity). In most natural systems, Pm is either very large or very small. The former limit is appropriate for hot diffuse plasmas such as the warm and hot phases of the interstellar medium and the intracluster medium of galaxy clusters. The latter limit is realized in denser environments, e.g., the liquid-metal cores of planets ($Pm \sim 10^{-5}$), the stellar convective zones ($Pm \sim 10^{-7} - 10^{-4}$ for the Sun, depending on the depth), and protostellar discs. In liquid-sodium experiments, where $Pm \sim 10^{-6}$, the main problem has been to access the high- Rm regime: thus, to get $Rm \sim 10^2$, it is necessary to drive fluid flows with $Re \sim 10^8$.

The importance of Pm lies in that it determines the relative size of the viscous and resistive scales in the system (denoted here l_ν and l_η , respectively). When $Pm \gg 1$, $l_\eta/l_\nu \sim Pm^{-1/2} \ll 1$ for a weak growing field (i.e., in the kinematic-dynamo regime;

see Schekochihin, Cowley, Taylor, Maron & McWilliams 2004, and references therein). This means that the resistive scale lies outside the inertial range of the turbulence, deep in the viscous range, where the velocity field is spatially smooth. In contrast, when $Pm \ll 1$ (while both $Re \gg 1$ and $Rm \gg 1$), one expects $l_\eta/l_\nu \sim Pm^{-3/4} \gg 1$ (Moffatt 1961). This estimate places the magnetic cutoff in the middle of the inertial range, asymptotically far away both from the viscous and the outer scales. Thus, the computational challenge posed by large or small values of Pm is to resolve two scale separations: $L \gg l_\nu \gg l_\eta$ for $Pm \gg 1$ or $L \gg l_\eta \gg l_\nu$ for $Pm \ll 1$.

The fluctuation dynamo at large Pm is an easier case both to understand physically and to handle numerically. In this limit, field amplification is due to the random stretching of the magnetic field by the fluid motion (Batchelor 1950, Moffatt & Saffman 1963, Zeldovich et al. 1984, Childress & Gilbert 1995, Ott 1998, Chertkov et al. 1999). Since the spatially smooth viscous-scale motions have the largest turnover rate, they are primarily responsible for the stretching. It is, therefore, not essential to have a large Re in order to capture the field growth — all that is needed is a flow with chaotic trajectories, which can be spatially smooth (laminar). This simplification can be exploited to model numerically the large- Pm limit (Schekochihin, Cowley, Taylor, Maron & McWilliams 2004).

The case of $Pm = 1$, although not encountered in nature, has historically been the favourite choice of convenience in numerical simulations — it is, indeed, for this case that the fluctuation dynamo was first obtained in the computer (Meneguzzi et al. 1981). Examination of the nature of the dynamo at $Pm = 1$ leads one to conclude that it belongs essentially to the same class as the large- Pm limit (Schekochihin, Cowley, Taylor, Maron & McWilliams 2004). This is because the bulk of the magnetic energy in this case still resides below the viscous scale.

The physical considerations based on the random stretching that provide a qualitative (if not mathematically rigorous) explanation of how the fluctuation dynamo is possible (see references cited above) depend on the assumption that the scale of the fluid motion that does the stretching (the viscous scale l_ν) is larger than the scale of the field that is stretched (the resistive scale l_η). This cannot be valid in the case of low Pm , when $l_\eta \gg l_\nu$. Clearly, the latter limit is qualitatively different because the magnetic fluctuations, heavily dissipated below l_η , cannot feel the spatially smooth viscous-scale motions. Can the inertial-range and/or the outer-scale motions still make the field grow? No compelling *a priori* physical argument either for or against such a dynamo has been proposed. As was pointed out by Vainshtein (1982), in the absence of a better physical understanding, the problem is purely quantitative: the stretching and turbulent diffusion effects being of the same order at each scale in the inertial range, one cannot predict which of them wins.

Our first numerical investigation of the problem of low- Pm dynamo (Schekochihin, Cowley, Maron & McWilliams 2004) revealed that at fixed Rm , wherever there was dynamo at $Pm = 1$, it weakened or disappeared if Re was increased.¹ Our conclusion was

¹Previous attempts to simulate turbulent dynamo in various other, mostly convective, contexts

that, as far as we could tell at the resolutions available to us then, the critical magnetic Reynolds number Rm_c for dynamo increased with Re . This was confirmed by Haugen et al. (2004), who used a different (grid, rather than spectral) code. Our and their results, enhanced somewhat by using hyperviscosity, were assembled together by Schekochihin et al. (2005) to produce the first stability curve $Rm_c(Re)$ for the fluctuation dynamo. While we were able to show that Rm_c increased with Re , it remained unknown if this increase was to be eventually saturated with Rm_c reaching some finite limit as $Re \rightarrow \infty$. In this paper, we give a detailed report on the new results that show that it does, i.e., we demonstrate that *fluctuation dynamo at low Pm exists* (a preliminary report appeared in Isakov et al. (2007)). These results are described in section 2. We also report that the form of the magnetic-energy spectrum changes qualitatively in the low- Pm limit (section 2.4). We further discuss the comparison of our results with simulations by Ponty et al. (2006), Mininni (2007) and others of the fluctuation dynamo in turbulence with a mean flow (section 2.5) and discuss the remaining theoretical uncertainties and unsolved questions (section 2.6). The most important of these is whether the dynamo we have found is driven by the inertial-range motions at the resistive scale — if it is, its growth rate should be proportional to $Rm^{1/2}$, which would make it a dominant (and universal) field-amplification effect. Finally, we proceed in section 3 to report a numerical study of small-scale magnetic induction, an effect that is related rather closely to the dynamo problem. Section 4 summarizes our findings.

2. Fluctuation Dynamo

2.1. Problem Set Up

We use the standard pseudospectral method to solve in a periodic cube the equations of incompressible MHD:

$$\frac{\partial \mathbf{u}}{\partial t} + \mathbf{u} \cdot \nabla \mathbf{u} = -\nabla p - \nu_n |\nabla|^n \mathbf{u} + \mathbf{B} \cdot \nabla \mathbf{B} + \mathbf{f}, \quad (1)$$

$$\frac{\partial \mathbf{B}}{\partial t} + \mathbf{u} \cdot \nabla \mathbf{B} = \mathbf{B} \cdot \nabla \mathbf{u} + \eta \nabla^2 \mathbf{B}. \quad (2)$$

Here \mathbf{u} is the velocity field, \mathbf{B} is the magnetic field (in velocity units) and the density of the fluid is taken to be constant and equal to 1. In order to study the field growth or decay in the kinematic regime, we initialize our simulations with random magnetic fluctuations at very small energy — usually between 10^{-10} and 10^{-6} of the dynamically significant level — so the Lorentz force, while retained, is never important. The velocity is forced by a *nonhelical* homogeneous body force, which consists in randomly injecting energy in a δ -correlated (white-noise) fashion into the Fourier harmonics with wave numbers $|\mathbf{k}| \leq \sqrt{2} k_0$, where $k_0 = 2\pi$ is the box wave number (the box size is 1). The white-noise character of the forcing allows us to fix the average injected power per unit volume: $\varepsilon = \langle \mathbf{u} \cdot \mathbf{f} \rangle = 1$, where the angle brackets stand for volume and time averaging.

had also found achieving a sustained field amplification problematic at $Pm < 1$ (e.g., Nordlund et al. 1992, Brandenburg et al. 1996, Christensen et al. 1999).

Table 1. Index of runs — Part I

| Run | Res. | n | ν_n | Rm | Pm | Re | Re_λ | γ | u_{rms} | Fig. |
|---------------------------|---------|-----|-----------------------|------|---------|------|--------------|----------|------------------|---------------------------|
| $\eta = 4 \times 10^{-3}$ | | | | | | | | | | |
| a0 | 64^3 | 2 | 4×10^{-3} | 51 | 1.0 | 51 | 34 | -0.20 | 1.29 | 1 |
| H01 | 128^3 | 8 | 10^{-12} | 57 | 0.43 | 133 | 64 | -0.145 | 1.43 | 1, 6(a) |
| H02 | 128^3 | 8 | 10^{-14} | 57 | 0.180 | 320 | 98 | -0.89 | 1.43 | 1, 6(b) |
| H03 | 128^3 | 8 | 10^{-16} | 57 | 0.080 | 710 | 148 | -1.13 | 1.43 | 1, 6(d) |
| H04 | 128^3 | 8 | 10^{-17} | 57 | 0.052 | 1100 | 184 | -1.04 | 1.43 | 1, 6(e) |
| H05 | 256^3 | 8 | 10^{-18} | 57 | 0.034 | 1680 | 230 | -1.02 | 1.44 | 1, 6(f) |
| H07 | 256^3 | 8 | 10^{-20} | 57 | 0.0148 | 3800 | 342 | -0.99 | 1.43 | 1, 8(a) |
| $\eta = 2 \times 10^{-3}$ | | | | | | | | | | |
| A1 | 128^3 | 2 | 2×10^{-3} | 107 | 1.0 | 107 | 53 | 0.30 | 1.35 | 1 |
| A2 | 128^3 | 2 | 10^{-3} | 110 | 0.5 | 220 | 80 | 0.139 | 1.39 | 1 |
| A3 | 256^3 | 2 | 5×10^{-4} | 110 | 0.25 | 440 | 111 | -0.22 | 1.38 | 1 |
| A4* | 256^3 | 2 | 2.5×10^{-4} | 104 | 0.125 | 830 | 148 | -0.52 | 1.31 | 1 |
| A5* | 256^3 | 2 | 1.25×10^{-4} | 106 | 0.0625 | 1700 | 230 | -0.74 | 1.33 | 1 |
| A6* | 512^3 | 2 | 6.25×10^{-5} | 105 | 0.03125 | 3400 | 322 | -0.41 | 1.32 | 1, 4 |
| HA1 | 128^3 | 8 | 10^{-14} | 112 | 0.36 | 310 | 95 | 0.0106 | 1.41 | 1, 6(a) |
| HA2 | 128^3 | 8 | 10^{-16} | 112 | 0.157 | 710 | 144 | -0.64 | 1.40 | 1, 6(b) |
| HA3 | 128^3 | 8 | 10^{-17} | 109 | 0.109 | 1000 | 165 | -0.60 | 1.38 | 1, 6(d) |
| HA4 | 256^3 | 8 | 10^{-18} | 114 | 0.069 | 1660 | 220 | -0.54 | 1.43 | 1, 6(e) |
| HA6 | 256^3 | 8 | 10^{-20} | 117 | 0.030 | 3900 | 360 | -0.46 | 1.47 | 1, 4, 6(f), 8(a) |
| HA8* | 512^3 | 8 | 10^{-22} | 109 | 0.0173 | 6300 | 420 | -0.45 | 1.38 | 1 |
| $\eta = 10^{-3}$ | | | | | | | | | | |
| B1 | 128^3 | 2 | 10^{-3} | 210 | 1.0 | 210 | 80 | 0.77 | 1.34 | 1, 3(a) |
| B2 | 256^3 | 2 | 5×10^{-4} | 220 | 0.5 | 440 | 110 | 0.49 | 1.38 | 1, 3(a) |
| B3 | 256^3 | 2 | 2.5×10^{-4} | 230 | 0.25 | 900 | 160 | 0.161 | 1.42 | 1, 3(a) |
| B4 | 256^3 | 2 | 1.25×10^{-4} | 220 | 0.125 | 1760 | 230 | -0.141 | 1.38 | 1, 3(a) |
| B5* | 512^3 | 2 | 6.25×10^{-5} | 220 | 0.0625 | 3600 | 330 | -0.021 | 1.41 | 1, 3(a), 4, 5 |
| HB1 | 128^3 | 8 | 10^{-16} | 220 | 0.32 | 700 | 143 | 0.20 | 1.41 | 1, 3(b), 6(a) |
| HB2 | 128^3 | 8 | 10^{-17} | 230 | 0.21 | 1100 | 183 | -0.158 | 1.43 | 1, 6(b) |
| HB3* | 256^3 | 8 | 10^{-18} | 220 | 0.146 | 1490 | 200 | -0.31 | 1.37 | 1, 3(b), 6(c) |
| HB4 | 256^3 | 8 | 10^{-19} | 230 | 0.090 | 2500 | 280 | -0.129 | 1.44 | 1, 6(d) |
| HB5 | 256^3 | 8 | 10^{-20} | 230 | 0.057 | 4000 | 360 | -0.098 | 1.45 | 1, 3(b), 4, 5, 6(e), 8(a) |
| HB7* | 512^3 | 8 | 10^{-22} | 220 | 0.033 | 6700 | 450 | 0.089 | 1.40 | 1, 3(b), 6(f) |

In order to increase the range of Reynolds numbers amenable to computation at a finite resolution, we make use both of the Laplacian viscosity ($n = 2$ in (1)) and of the 8th-order hyperviscosity ($n = 8$). For the hyperviscous runs, we define the effective viscosity

$$\nu_{\text{eff}} = \frac{\varepsilon}{\langle |\nabla \mathbf{u}|^2 \rangle}. \quad (3)$$

Using the hyperviscosity appears to be a sensible way of treating the $Pm \ll 1$ limit because in this limit, the magnetic cutoff scale is much larger than the (hyper)viscous scale, $l_\eta \gg l_\nu$, and the magnetic properties of the system should not depend on the

Table 2. Index of runs — Part II

| Run | Res. | n | ν_n | Rm | Pm | Re | Re_λ | γ | u_{rms} | Fig. |
|-----------------------------|---------|---|-----------------------|------|-------|------|--------------|----------|------------------|------------------|
| $\eta = 7.5 \times 10^{-4}$ | | | | | | | | | | |
| HX1 | 256^3 | 8 | 10^{-17} | 300 | 0.28 | 1050 | 175 | 0.178 | 1.41 | 1(b), 6(a) |
| HX2 | 256^3 | 8 | 10^{-18} | 310 | 0.176 | 1760 | 240 | -0.033 | 1.46 | 1(b), 6(b) |
| HX4 | 256^3 | 8 | 10^{-20} | 310 | 0.087 | 3600 | 340 | -0.054 | 1.46 | 1(b), 6(d) |
| $\eta = 5 \times 10^{-4}$ | | | | | | | | | | |
| C1 | 256^3 | 2 | 5×10^{-4} | 440 | 1.0 | 440 | 111 | 1.40 | 1.39 | 1, 2, 3(c) |
| C2 | 256^3 | 2 | 2.5×10^{-4} | 430 | 0.5 | 870 | 159 | 0.89 | 1.36 | 1, 3(c) |
| C3 | 256^3 | 2 | 1.25×10^{-4} | 440 | 0.25 | 1760 | 230 | 0.49 | 1.38 | 1, 3(c) |
| C4* | 512^3 | 2 | 6.25×10^{-5} | 450 | 0.125 | 3600 | 360 | 0.21 | 1.42 | 1, 3(c), 4 |
| HC1 | 256^3 | 8 | 10^{-18} | 450 | 0.28 | 1620 | 220 | 0.43 | 1.41 | 1, 3(d), 6(a) |
| HC2 | 256^3 | 8 | 10^{-19} | 450 | 0.183 | 2500 | 270 | 0.20 | 1.42 | 1, 6(b) |
| HC3 | 256^3 | 8 | 10^{-20} | 470 | 0.110 | 4300 | 380 | 0.120 | 1.48 | 1, 3(d), 4, 6(c) |
| HC4* | 512^3 | 8 | 10^{-21} | 460 | 0.090 | 5100 | 400 | 0.27 | 1.44 | 1, 6(d) |
| HC5* | 512^3 | 8 | 10^{-22} | 430 | 0.070 | 6200 | 410 | 0.26 | 1.36 | 1, 2, 3(d), 6(e) |
| $\eta = 2.5 \times 10^{-4}$ | | | | | | | | | | |
| D1* | 512^3 | 2 | 2.5×10^{-4} | 810 | 1.0 | 810 | 141 | 1.85 | 1.27 | 1 |
| D2* | 512^3 | 2 | 1.25×10^{-4} | 830 | 0.5 | 1660 | 210 | 1.41 | 1.31 | 1 |
| D3* | 512^3 | 2 | 6.25×10^{-5} | 830 | 0.25 | 3300 | 320 | 0.91 | 1.31 | 1, 4 |
| HD1* | 512^3 | 8 | 10^{-20} | 900 | 0.24 | 3800 | 340 | 0.80 | 1.42 | 1, 4, 6(a) |
| HD3* | 512^3 | 8 | 10^{-22} | 850 | 0.145 | 5900 | 390 | 0.59 | 1.34 | 1, 6(c) |

particular form of the viscous cutoff. In our earlier work (Schekochihin et al. 2005), it was confirmed that, as far as the values of Rm_c are concerned, this is approximately true for a number of different choices of the viscous regularization, including the 4th-, 6th-, and 8th-order hyperviscosity and the Smagorinsky LES viscosity (see further discussion in section 2.3). It is the effective viscosity given by (3) that is used for calculating Re and Pm in the hyperviscous runs. Thus, we define

$$Rm = \frac{\sqrt{\langle |\mathbf{u}|^2 \rangle}}{\eta k_0}, \quad Pm = \frac{\nu}{\eta}, \quad Re = \frac{\sqrt{\langle |\mathbf{u}|^2 \rangle}}{\nu k_0}, \quad Re_\lambda = \frac{1}{\nu} \sqrt{\frac{5}{3} \frac{\langle |\mathbf{u}|^2 \rangle^2}{\langle |\nabla \mathbf{u}|^2 \rangle}}, \quad (4)$$

where $\nu = \nu_2$ for the Laplacian runs and $\nu = \nu_{\text{eff}}$ for the hyperviscous ones. We follow an established convention by using the box wave number $k_0 = 2\pi$ in the definitions of Rm and Re . A characteristic of turbulence independent of this choice is Re_λ , the Reynolds number based on the Taylor microscale (also defined above).

The maximum resolution that we could afford was 512^3 . All our runs are summarized in table 1 and table 2, where we give for each run its resolution, the values of the (hyper)viscosity ν_n , Rm , Pm , Re , Re_λ , the growth/decay rate γ , the rms velocity $u_{\text{rms}} = \sqrt{\langle |\mathbf{u}|^2 \rangle}$, and a list of figures in which this run appears. The runs marked with a star were done using a new code written by A. Iskakov. All other runs were done using another code, written by J. Maron, which was the code used in our earlier papers

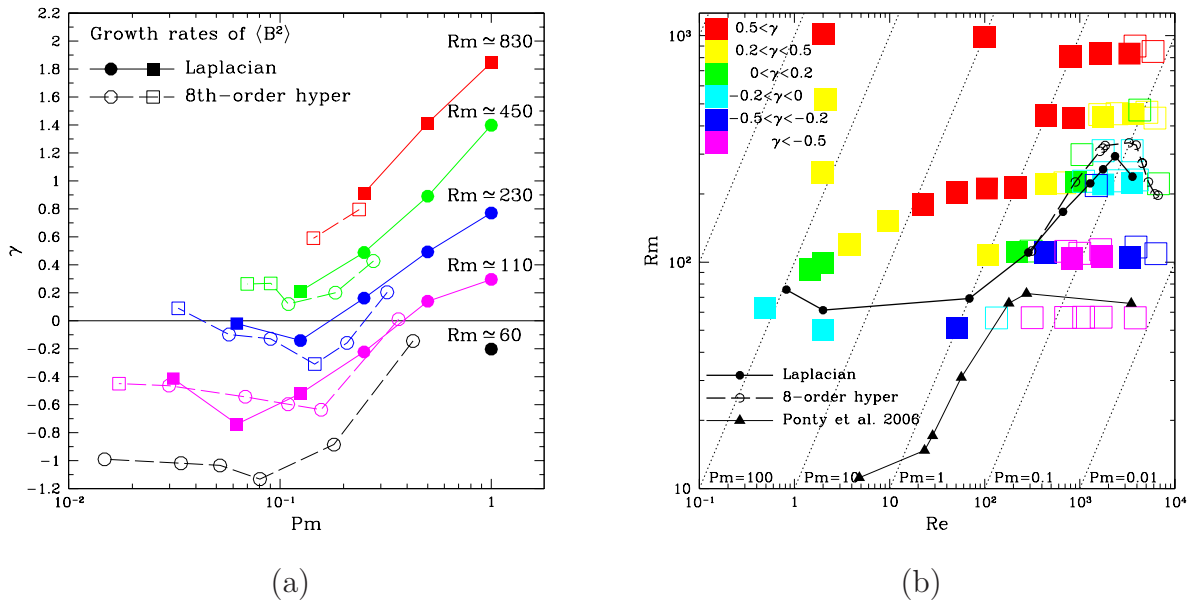


Figure 1. (a) Growth/decay rate of $\langle |B|^2 \rangle$ vs. Pm for five values of Rm ($Rm \sim 60$: run a0 and series H0; $Rm \sim 110$: series A and HA ; $Rm \sim 230$: series B and HB; $Rm \sim 450$: series C and HC; $Rm \sim 830$: series D and HD). The round points were obtained using the code written by J. Maron, the square points using the code written by A. Iskakov. The unit of the growth rate is approximately one inverse turnover time at the outer scale (the precise units of time are set by $\varepsilon = 1$ and the box size = 1.) (b) Growth/decay rates in the parameter space (Re , Rm). The filled points correspond to runs with Laplacian viscosity, the empty ones to runs with 8th-order hyperviscosity. The interpolated stability curves $Rm_c(Re)$ based on the Laplacian and hyperviscous runs are shown separately. For comparison, we also plot the $Rm_c(Re)$ curve obtained by Ponty et al. (2006) for the turbulence with a mean flow (see section 2.5 for discussion).

(Schekochihin, Cowley, Taylor, Maron & McWilliams 2004, Schekochihin, Cowley, Maron & McWilliams 2004, Schekochihin et al. 2005). Both codes are pseudospectral, solve the same equations ((1) and (2)) and use the same units of length and time, but different time-stepping, FFT and parallelisation algorithms, as well as slightly different implementations of the random forcing. We have checked conclusively that A. Iskakov’s code correctly reproduces the older results obtained with J. Maron’s code.

2.2. Results: Existence of the Dynamo

In figure 1(a), we show the growth/decay rates of the magnetic energy $\langle |B|^2 \rangle$ vs. Pm for five sequences of runs. The runs in each sequence have the same fixed value of η and, consequently, approximately the same value of Rm . Thus, decreasing Pm in each of these sequences is achieved by increasing Re while keeping Rm fixed. This is the same strategy as was employed by Schekochihin, Cowley, Maron & McWilliams (2004). Figure 1(a) extends their figure 1(b), which showed runs A1–A3 and B1–B4.

The growth rates are calculated via a least-squares fit to the evolution of $\ln(\langle |B|^2 \rangle)$

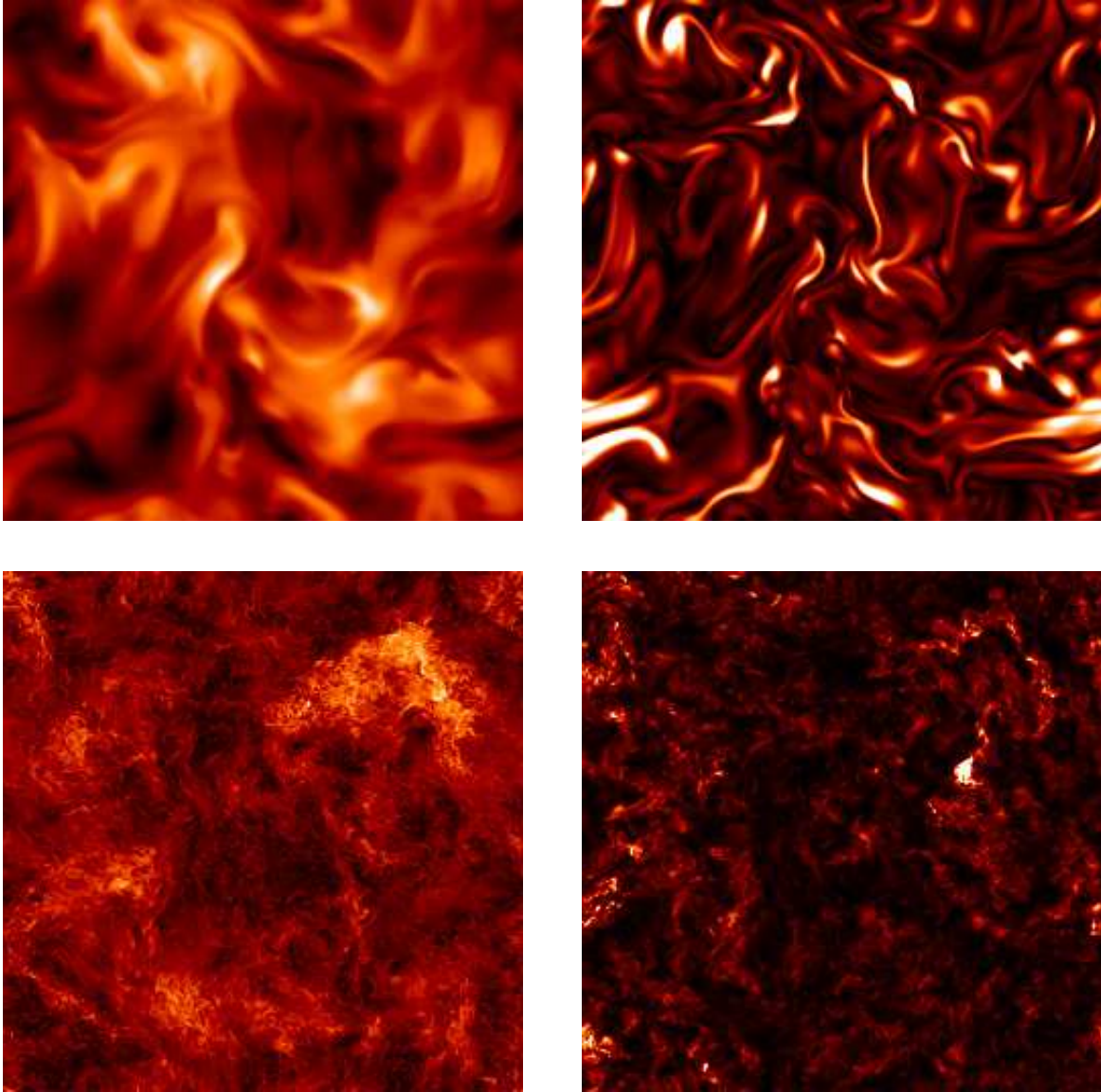


Figure 2. Cross-sections of the absolute values of the velocity (left) and the (growing) magnetic field (right) for two runs with similar Rm : run C1, $Rm = Re \simeq 440$ (top) and run HC5, $Rm \simeq 430$, $Re \simeq 6200$ (bottom). The lighter/darker regions correspond to stronger/weaker fields.

vs. time. The run times were chosen so that a converged value of the growth/decay rate could be obtained. In most cases, this requires no more than 10 to 20 box-crossing times, although for near-marginal cases ($|\gamma| \lesssim 0.1$; see table 1 and table 2), the convergence is quite poor. This is because close to criticality, the evolution of the total magnetic energy has very long time correlations, with long periods of virtually zero change punctuated by periods of growth or decay. Fitting such a time evolution to a single growth/decay rate is not a particularly precise operation.

The trend manifested in figure 1(a) is clear: as Pm is decreased, the growth rate

decreases, passes through a minimum and then saturates at a constant value, i.e.,

$$\gamma(Rm, Re) \rightarrow \gamma_\infty(Rm) = \text{const as } Re \rightarrow \infty \text{ and } Rm \text{ is fixed.} \quad (5)$$

That such a limit should exist is natural because as $Re \rightarrow \infty$ at fixed Rm , we have $l_\eta \gg l_\nu \sim LRe^{-3/4} \rightarrow 0$ and one cannot expect the magnetic field to “know” exactly how small the viscous cutoff scale is. A much more significant result is that as Rm increases, the entire curve $\gamma(Re, Rm)$ is lifted upwards, so both the minimum and the asymptotic value of γ are positive for $Rm \sim 450$ and above. For $Rm \sim 230$, γ becomes negative approximately at $Pm \sim 0.2$ but the curve crosses zero again at $Pm \sim 0.03$ and emerges on the positive side, so the asymptotic value is expected to be positive. While we are unable at current resolutions to obtain the asymptotic values of γ for the growing cases, we consider the evidence presented in figure 1(a) sufficient to claim that such values exist and are positive.

Thus, the fluctuation dynamo does exist in the nonhelical turbulence of conducting fluid with low Pm . It is perhaps interesting to have a glimpse of what this turbulence “looks like.” Snapshots of the velocity and the growing magnetic field for a run (HC5) with $Pm \simeq 0.07$ and $Rm \simeq 430$ are shown in figure 2 and contrasted with similar snapshots for a run (C1) that has approximately the same value of $Rm \simeq 440$ but $Pm = 1$ and in which the magnetic field exhibits a folded structure characteristic of the fluctuation dynamo at $Pm \geq 1$ (Schekochihin, Cowley, Taylor, Maron & McWilliams 2004, Brandenburg & Subramanian 2005, Wilkin et al. 2007).

Figure 1(b) presents the magnetic-energy growth/decay rates in the two-dimensional parameter space (Re, Rm) . We also include the growth/decay rates for the $Pm \geq 1$ runs published in Schekochihin, Cowley, Maron & McWilliams (2004) and Schekochihin, Cowley, Taylor, Maron & McWilliams (2004) to give a complete picture of what is known about the dependence $\gamma(Re, Rm)$ (these runs are not shown in table 1 and table 2). We are now able to reconstruct the stability curve $Rm_c(Re)$: each point on the curve is a linear interpolation between a decaying and a growing case (this is done separately for the Laplacian and hyperviscous runs). We see that Rm_c increases with Re , reaches a maximum around $Rm_c^{(\text{max})} \sim 350$ and $Re \sim 3000$, and then decreases (rather sharply). We expect that

$$Rm_c(Re) \rightarrow Rm_c^{(\infty)} = \text{const as } Re \rightarrow \infty, \quad (6)$$

again on the grounds that exactly where the viscous cutoff is cannot matter in this limit, but we cannot as yet obtain the asymptotic value $Rm_c^{(\infty)}$. Discounting the unlikely possibility that the stability curve has multiple extrema at larger Re , we expect the asymptotic value to be $Rm_c^{(\infty)} \lesssim 200$. Above this value of Rm , there is always dynamo action at small enough Pm . Note that this represents an increase of only about a factor of 3 compared to the well-known critical value $Rm_c \simeq 60$ for the fluctuation dynamo at $Pm \geq 1$ (established first by Meneguzzi et al. (1981) and confirmed in many subsequent numerical studies, e.g., Schekochihin, Cowley, Taylor, Maron & McWilliams (2004), Haugen et al. (2004)).

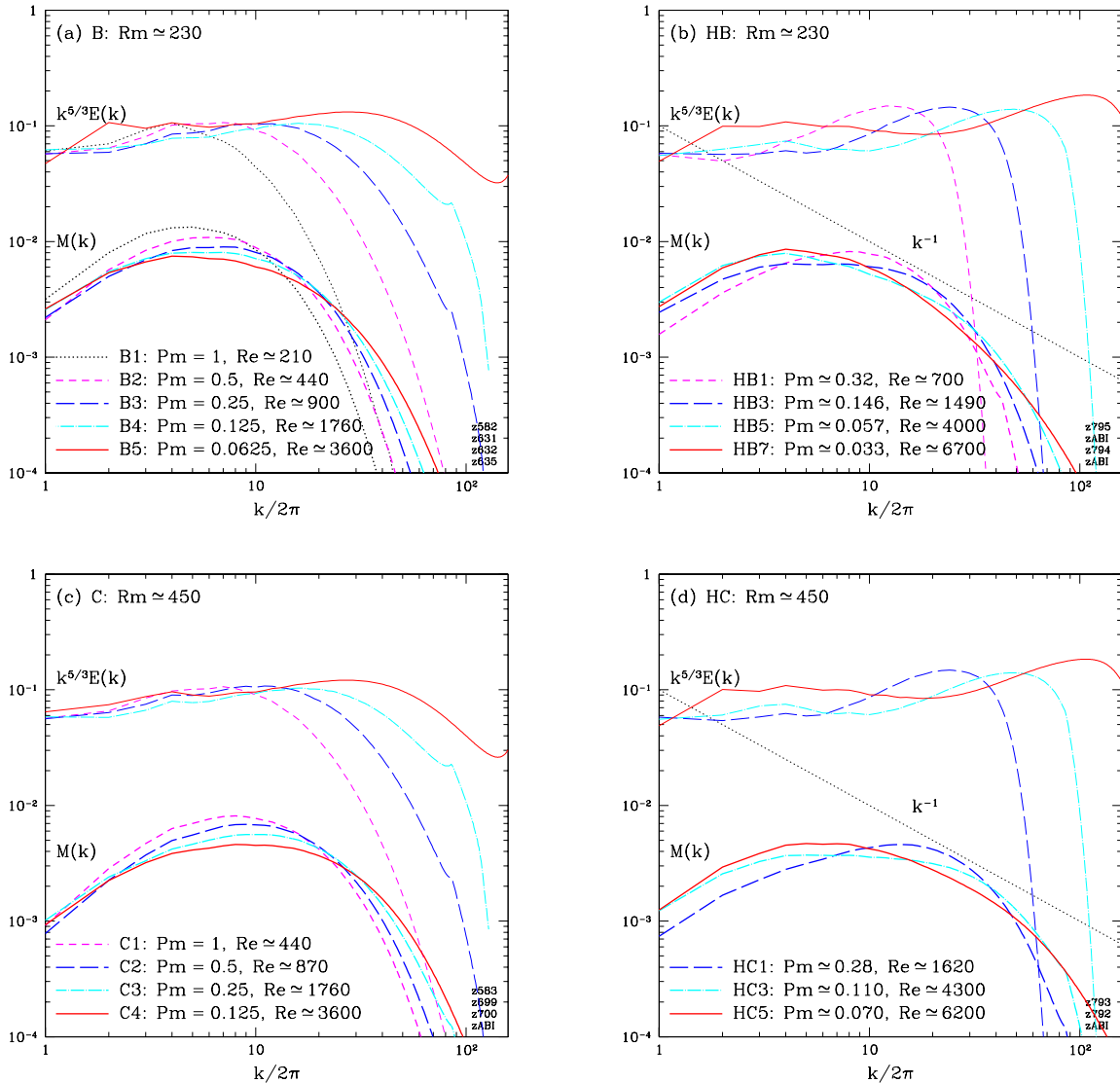


Figure 3. Spectra of the kinetic energy (normalized by $\langle |\mathbf{u}|^2 \rangle / 2$, time-averaged and compensated by $k^{5/3}$) and of the magnetic energy (normalized at each time by the instantaneous value of $\langle |\mathbf{B}|^2 \rangle / 2$ and time-averaged) for the kinematic decaying/growing cases with fixed Rm and increasing Re : (a) B series (Laplacian, $Rm \sim 230$), (b) HB series (hyperviscous, $Rm \sim 230$), (c) C series (Laplacian, $Rm \sim 450$), (d) HC series (hyperviscous, $Rm \sim 450$). In all of these cases, $\langle |\mathbf{B}|^2 \rangle \ll \langle |\mathbf{u}|^2 \rangle$. The k^{-1} slope is given for reference and discussed in section 3.2.

Figure 1(b) extends figure 2 of Schekochihin et al. (2005), who could only see the increasing part of the curve. They also reported the $Rm_c(Re)$ dependence obtained from the Laplacian, 6th-order hyperviscous and Smagorinski-LES simulations using the grid-based PENCIL code. While the low- Pm fluctuation dynamo has yet to be found using this code, a comparison with figure 1(b) shows that the (presumed) maximum of the stability curve for the PENCIL-code dynamo should lie significantly above the value we have found in our simulations: apparently at $Rm_c^{(\max)} \gtrsim 500$ and $Re \gtrsim 3000$. This raises

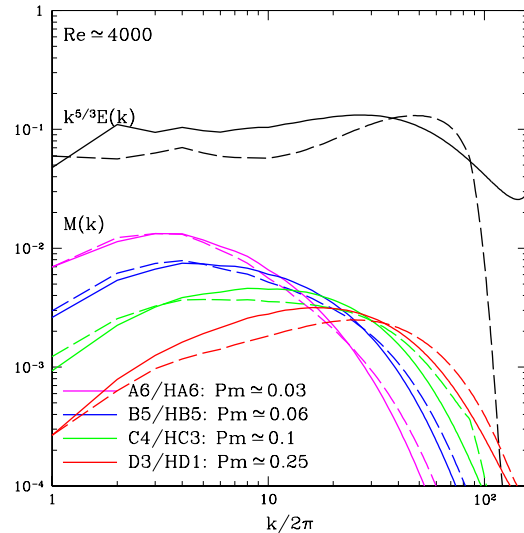


Figure 4. Spectra of the kinetic and magnetic energies (normalized as in figure 3) for the kinematic decaying/growing cases with fixed $Re \simeq 4000$ and different Pm . For each value of Rm , we plot the spectra for a Laplacian (solid lines) and a hyperviscous (dashed lines) run. The kinetic-energy spectra are independent of Rm .

the question of how universal the results we are reporting are. Another piece of numerical evidence that leads to the same question is the (small but measurable) difference between the stability curves reconstructed using the Laplacian and the hyperviscous runs.

2.3. Laplacian vs. Hyperviscous Simulations

As we argued in the Introduction, it is reasonable to assume that whether or not the dynamo action is present in the limit of $Rm \ll Re \rightarrow \infty$ does not depend on the nature of the viscous cutoff. If this is true, demonstrating that it is present in the hyperviscous case should be sufficient to claim that it is present generally. It is also likely that the asymptotic value $Rm_c^{(\infty)}$ will prove to be robust. However, the *shape* of the stability curve $Rm_c(Re)$ is certainly not universal. Indeed, let us consider what determines this shape in the transition region between $Rm_c \simeq 60$ for $Pm \geq 1$ and the yet undetermined asymptotic value $Rm_c^{(\infty)} \lesssim 200$ for $Pm \ll 1$. When $Re \leq Rm$ ($Pm \geq 1$), the viscous scale is larger than the resistive one, $l_\nu > l_\eta$. As Re is increased compared to Rm , the viscous scale decreases and eventually becomes smaller than the resistive scale. At the intermediate values of Re , the resistive scale finds itself transiting the spectral bottleneck associated with the viscous cutoff until it eventually emerges into the inertial range. This transition is illustrated by figure 3, which shows the spectra of the kinetic and magnetic energies for two of the fixed- Rm sequences of runs whose growth rates were shown in figure 1(a). It is obvious that the properties of the velocity field around the viscous scale do depend on the type of viscous dissipation employed. Therefore, the curves $\gamma(Re, Rm)$ and $Rm_c(Re)$ cannot be universal around the transitional values of

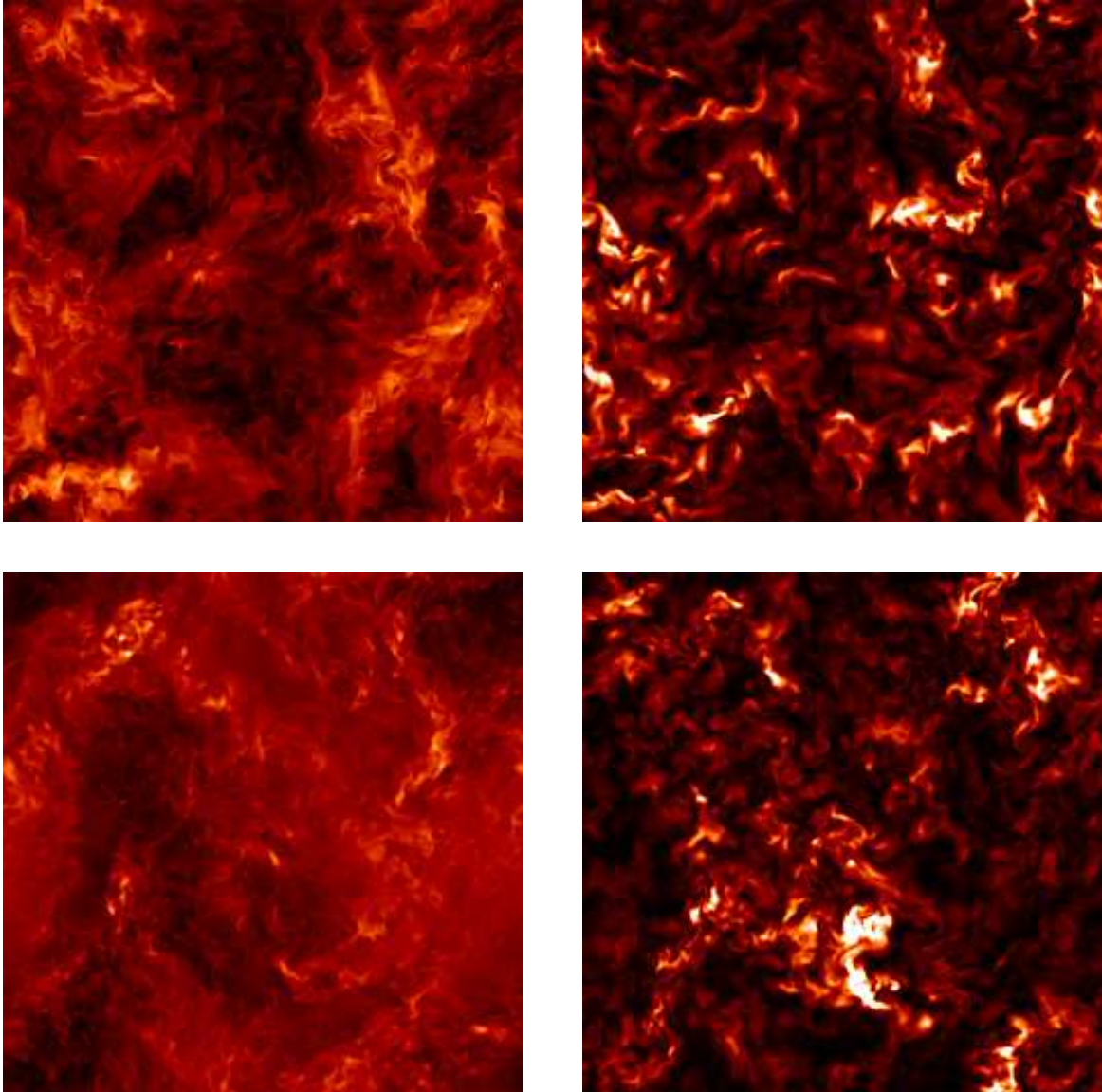


Figure 5. Cross-sections of the absolute values of the velocity (left) and the magnetic field (right) for a Laplacian run (B5, top) and a hyperviscous run (HB5, bottom), both with $Rm \sim 200$ and $Re \sim 4000$. Note that these runs are near-marginal with respect to the field growth (see table 1 and figure 1(a)).

Re and Rm . In particular, since the bottleneck region is narrower in the wave-number space for the hyperviscous runs (see figure 3), we expect that so is the transition region in the parameter space.²

The degree to which the properties of the magnetic field in the Laplacian and

²For the PENCIL-code runs in Schekochihin et al. (2005), the relatively higher values of Rm and Re at which the transition seems likely to occur may also be due to the generally more dissipative character of a grid code compared to the pseudospectral ones. Another possible source of nonuniversality might be the difference between the forcing schemes — if the dynamo is controlled by the outer-scale motions, a possibility discussed at the end of section 2.6.

hyperviscous runs become similar in the limit $Re \gg Rm \gg 1$ can be judged from figure 4, where we show the magnetic-energy spectra corresponding to the same value of $Re \sim 4000$ and four different values of Pm . For each value of Pm , the spectra obtained in a Laplacian and a hyperviscous run are given. As Pm decreases, the bulk of the magnetic energy is separated in the wave-number space from the nonuniversal viscous cutoff and the magnetic-energy spectra in the Laplacian and hyperviscous runs resemble each other more.

Figure 5 gives a visual illustration of the Laplacian vs. hyperviscous simulations at low Pm . We show snapshots of the velocity and magnetic field in two such runs (C4 and HC3) with similar values of $Rm \sim 200$ and $Re \sim 4000$. While some differences in the velocity structure are visible, the magnetic fields look very similar.

The growth/decay rates for the Laplacian and hyperviscous runs with similar Rm and Re are also quite close. The entire curves $\gamma(Pm)$ can only be meaningfully compared for two of the run sequences shown in figure 1(a): $Rm \sim 110$ (series A vs. series HA) and $Rm \sim 230$ (series B vs. series HB). Away from the transition region, they appear to agree quite well. Further evidence in favour of the equivalence of the Laplacian and hyperviscous runs at $Re \gg Rm \gg 1$ is provided by the agreement between saturated energies of the induced magnetic fluctuations in such runs (see section 3.2).

2.4. Results: Magnetic-Energy Spectra

In examining figure 3, it is hard not to notice that the shape of the magnetic-energy spectrum changes as Re is increased. At Pm above and just below unity, the spectrum has a positive slope and its peak is at the resistive scale. This is a typical situation for the fluctuation dynamo at $Pm \geq 1$ — in the limit $Pm \gg 1$, a $k^{+3/2}$ spectrum is expected, known as the Kazantsev (1968), or Kulsrud & Anderson (1992), spectrum. As the system enters the low- Pm regime, the spectral slope flattens and then becomes negative. Since this is a qualitative change and since, as far as we know, such spectra have not been seen before, it is worth documenting them in more detail.

The series of plots presented in figure 6 illustrates how the magnetic-energy spectrum depends on Pm . In each of these plots, we have assembled together the spectra for runs with different Rm and Re whose ratio was approximately equal to a chosen fixed value of Pm — approximately because for the hyperviscous case, one cannot fix Pm exactly before performing the simulation (see (3) and (4)). Making allowances for this imprecision, it is still possible to conclude tentatively from figure 6 that the slope of the magnetic-energy spectrum depends on Pm but not on individually on Re or Rm . As Pm decreases, the slope turns from positive to negative. The data appears more consistent with the peak of the spectrum shifted towards the outer scale than with it moving with the resistive scale ($l_\eta \sim LRm^{-3/4}$; see section 2.6), but again, this is only a tentative conclusion.

Unfortunately, here as everywhere else, an attempt to establish numerically a solid asymptotic result is frustrated by the resolution constraints: in order to determine

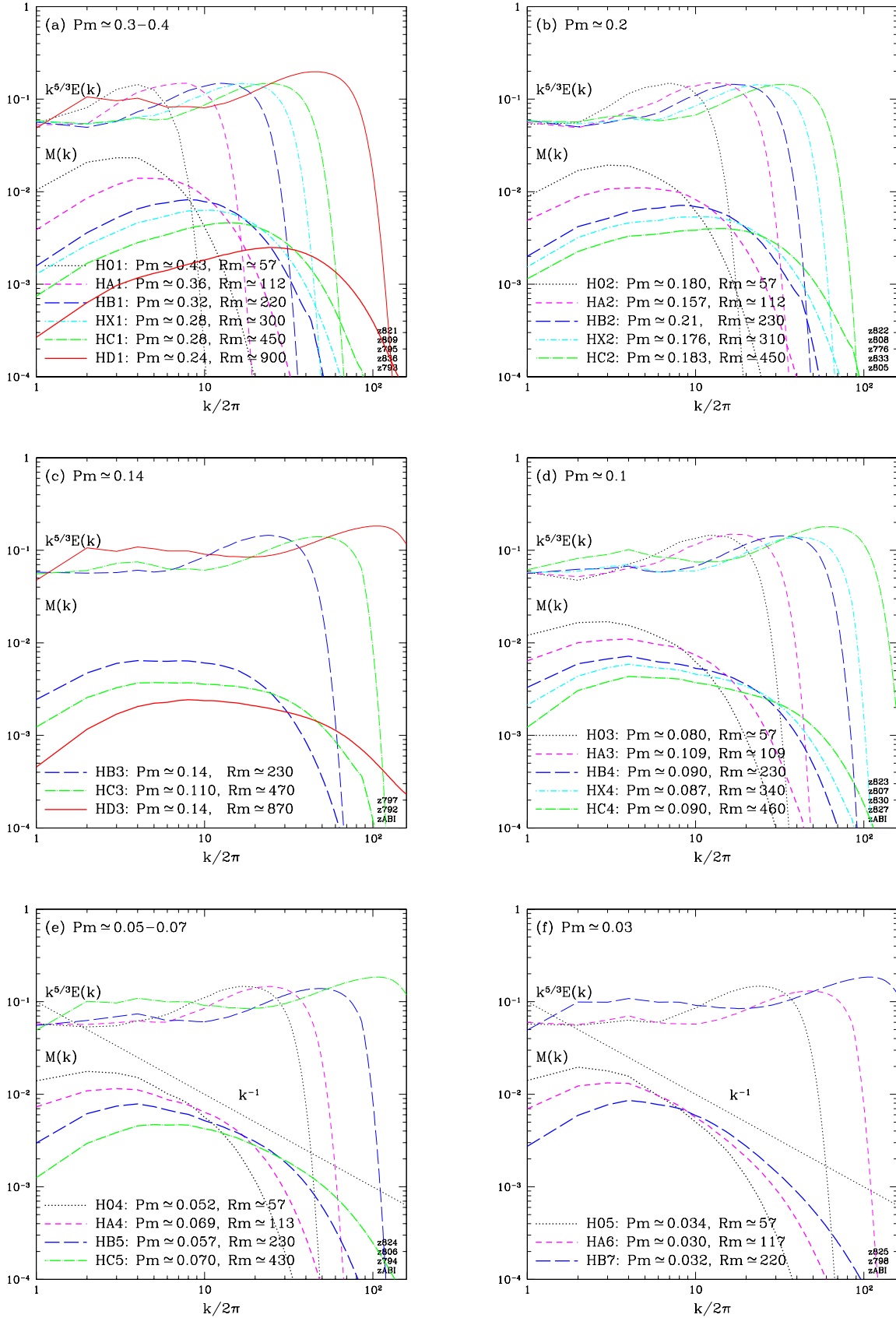


Figure 6. Spectra of the kinetic and magnetic energies (normalized as in figure 3) for the kinematic decaying/growing cases with (approximately) fixed Pm : (a) $Pm \approx 0.3 - 0.4$, (b) $Pm \approx 0.2$, (c) $Pm \approx 1.4$, (d) $Pm \approx 0.1$, (e) $Pm \approx 0.05 - 0.07$, (f) $Pm \approx 0.03$. The dashed lines are for the growing cases and the solid lines are for the decaying cases.

the spectral slope or the position of the spectral peak, we need to resolve the limit $Re \gg Rm \gg 1$ (i.e., both $Pm \ll 1$ and $Rm \gg 1$), but we cannot currently achieve sufficiently large values of Rm for $Pm \ll 1$. We shall, therefore, not make any final statements here about the asymptotic form of the magnetic spectrum, although in figure 6(e,f) we did provide the reference slope of k^{-1} and will discuss it as a theoretical possibility in section 3.2.

Note finally that the form of the spectrum does not change qualitatively between the growing and decaying runs: for example, in figure 6(c), the magnetic energy in run HB3 decays while in runs HC3 and HD3 it grows, but the spectral slope appears to be the same.

2.5. Discussion: Relation to Results for Turbulence with a Mean Flow

Since we have claimed above that the low- Pm fluctuation dynamo had not previously been seen in numerical simulations, it is important to explain how our results should be compared with the $Rm_c(Re)$ dependences obtained in the recent numerical studies by Nore et al. (1997), Ponty et al. (2005), Mininni, Ponty, Montgomery, Pinton, Politano & Pouquet (2005), Ponty et al. (2006), Laval et al. (2006), Mininni & Montgomery (2005), Mininni (2006) and Mininni (2007). In their simulations, turbulence was forced not by a random large-scale white noise, but by an imposed body force constant in time (a Taylor-Green forcing in the first five references, an ABC forcing in the other three). This produces a mean flow, i.e., a constant (mostly large-scale) spatially inhomogeneous velocity field that persists under averaging over times far exceeding its own turnover time. There is also a fluctuating multiscale velocity field (turbulence), which coexists with the mean flow and is energetically a few times weaker than it. Together, the mean flow plus the turbulence are a nonlinear solution of the Navier-Stokes equation (1) with constant forcing. The primary motivation for studying the dynamo properties of such a field is its close resemblance to the velocity field in liquid-metal dynamo experiments (e.g., Peffley et al. (2000), Spence et al. (2006), Monchaux et al. (2007)); the dynamo properties of the flows specific to these experiments have also been studied numerically: see, e.g., Ravelet et al. (2005), Bayliss et al. (2007)).

The mean flows that develop in such systems are usually dynamos by themselves — *mean-field dynamos*, to be precise (both in the case of helical mean flows like the ABC and in the nonhelical case of the Taylor-Green forcing). They give rise to growing magnetic fields at scales larger than the scale of the flow (or comparable to it, when the scale of the mean flow is comparable to the size of the simulation box). For $Pm \geq 1$, the threshold for the field amplification is very low in these systems: $Rm_c \sim 10$, which is a typical situation for the mean-field dynamos (cf. Galanti et al. 1992, Brandenburg 2001). The presence of a large amount of the small-scale magnetic energy in these simulations should most probably be attributed to the *magnetic induction*, rather than to the fluctuation dynamo, because the growth is happening at values of Rm that are well below the fluctuation-dynamo threshold ($Rm_c \sim 60$ for $Pm \geq 1$; see figure 1(b)).

As Pm is decreased, Rm_c increases and eventually saturates at some larger value, giving rise to a stability curve $Rm_c(Re)$ that looks similar to the stability curve we have obtained in our simulations. This similarity (enhanced sometimes by the ambiguity in the definitions of the Reynolds numbers) ought not to lead to any confusion between the two curves. In order to illustrate the difference between them, we have plotted in figure 1(b) the stability curve reported by Ponty et al. (2006) for their simulations with a Taylor-Green forcing. The data is taken from their table 1 and calibrated according to our definitions of Re and Rm : they define $Re = \sqrt{\langle |\mathbf{u}|^2 \rangle} L_{\text{dyn}}/\nu$, where L_{dyn} is the dynamical integral scale computed from the kinetic-energy spectrum and given in their table 1, while we define Re according to (4). The box wave number $k_0 = 1$ in their calculations. We see that the two curves are very different: the dynamo threshold for the simulations with a mean flow is much lower than for our homogeneous simulations. The difference is not merely quantitative: the ordered large-scale structure of the growing magnetic field in the $Pm \sim 1$ runs of Ponty et al. (2005) (the lower part of their stability curve) confirms that it is a mean-field dynamo.

The increase of Rm_c with increasing Re in these simulations has been attributed to the interference by the turbulence with the dynamo properties of the mean flow — a manifestation of a tendency for higher dynamo thresholds in the presence of a large-scale noise (Pétrélis & Fauve 2006, Laval et al. 2006). It would be interesting to check whether the turbulence in these simulations might itself act as a dynamo if the mean flow is “manually” removed from the induction equation (2). Comparison of the two stability curves in figure 1(b) suggests that in order for this to be the case, Rm must be increased very substantially — above the threshold found by us.

Let us conclude this discussion on a speculative note. While simulations with a mean flow undoubtedly exhibit a mean-field dynamo at $Pm \geq 1$, it is not clear whether that is also the case when $Pm \ll 1$. It may or may not be a coincidence that the low- Pm threshold for the simulations with a mean flow appears to be very close to the large- Pm fluctuation-dynamo threshold. Since the mean flow most probably has chaotic Lagrangian trajectories (although this has not been explicitly checked), it should be a fluctuation dynamo — it belongs to the same class as the large- Pm dynamos because the flow is spatially smooth. Could the turbulence, while suppressing the mean-field dynamo in the low- Pm regime, somehow fail to interfere with the fluctuation dynamo of the mean flow? There is not enough evidence or physical insight available to us to judge the merits of this possibility — or of another, equally speculative one that we float at the end of section 2.6. Two aspects of the published numerical results that seem to support it are the evidence of direct nonlocal transfer of energy from the outer scale (the mean flow) to the small-scale magnetic field (Mininni, Alexakis & Pouquet 2005) and the fact that the magnetic-energy spectra reported by Ponty et al. (2005) do not exhibit the tendency towards a negative slope discussed in section 2.4, but rather bear a strong resemblance to the typical $k^{+3/2}$ spectra of the fluctuation dynamo at $Pm \geq 1$ (see, e.g., Schekochihin, Cowley, Taylor, Maron & McWilliams 2004, Haugen et al. 2004).

2.6. Discussion: Relation to Theory and Outstanding Questions

Given the numerical certainty that the low- Pm fluctuation dynamo exists, there remain a number of theoretical uncertainties about the nature of this dynamo. The key question is whether or not it is the inertial-range motions that amplify the magnetic energy.

Suppose $Re \gg Rm \gg 1$. Let us examine what can be achieved by assuming that the transfer of the kinetic into magnetic energy is *local* in scale space.³ For Kolmogorov turbulence, the characteristic velocity fluctuation at scale l is $\delta u_l \sim (\varepsilon l)^{1/3}$, where ε is the total power injected into the turbulence (the turbulent energy flux). The characteristic rate of stretching of the magnetic field by the velocity field at scale l is then $\delta u_l/l \sim \varepsilon^{1/3} l^{-2/3}$. The characteristic rate of turbulent diffusion at scale l is of the same order. Comparing the stretching rate with the rate of the Ohmic diffusion of the magnetic field, η/l^2 , one finds the resistive scale, i.e., the scale at which the stretching rate is maximal and below which it is overcome by diffusion (Moffatt 1961):

$$l_\eta \sim \left(\frac{\eta^3}{\varepsilon} \right)^{1/4} \sim \frac{L}{Rm^{3/4}} \quad (7)$$

(this resistive scale does, indeed, lie inside the inertial range, $L \gg l_\eta \gg l_\nu$, where the viscous scale l_ν is estimated using (7) with η replaced by ν). Thus, if the local interaction of the inertial-range motions with the magnetic field is capable of amplifying the field in a sustained way, the growth rate of the magnetic energy should scale with Rm as

$$\gamma \sim \frac{\delta u_{l_\eta}}{l_\eta} \sim \frac{\varepsilon^{1/3}}{l_\eta^{2/3}} \sim \left(\frac{\varepsilon}{\eta} \right)^{1/2} \sim \frac{u_{\text{rms}}}{L} Rm^{1/2} \quad (8)$$

in the limit $Re \rightarrow \infty$. This dynamo, if it exists, is purely a property of the inertial range and is independent of any system-dependent outer-scale circumstances such as, e.g., the presence of a mean flow. Given a large enough Rm , the growth rate (8) will always be larger than a mean-field or any other kind of dynamo associated with the outer-scale motions, because the latter cannot amplify the field faster than at the rate

$$\gamma \sim \frac{U}{L} \sim \frac{u_{\text{rms}}}{L}, \quad (9)$$

where U is the characteristic velocity at the outer scale.

While our numerical results allowed us to make what we consider a compelling case for the existence of a positive asymptotic value of the growth rate (section 2.2), we cannot at this stage check whether it scales with Rm according to (8) or reaches an Rm -independent limit as in (9). Neither of these possibilities can be ruled out *a priori*.

Should the scaling (8) be confirmed, the case for an inertial-range dynamo would be complete. This case is strengthened somewhat by the theoretical predictions based

³Whether it really is local should be the subject of a thorough future investigation, possibly along the lines of the recent study by Mininni, Alexakis & Pouquet (2005) of a mean-flow-driven dynamo. Note that the shell-model simulations recently carried out by Stepanov & Plunian (2007), which enforce the locality of interactions, return a picture that seems to be broadly in agreement with the inertial-range dynamo scenario discussed below. On the other hand, EDQNM closure simulations do not find any increase in Rm_c for $Pm \ll 1$ compared with $Pm \geq 1$ (L  orat et al. 1981).

on the only available model of the turbulent dynamo that is solvable exactly — the Kazantsev (1968) model. This model considers a Gaussian random velocity field that is a white noise in time. The salient property of the inertial-range velocities is their spatial roughness: $\delta u_l \sim l^{1/3}$ for $L \gg l \gg l_\nu$ compared with a smooth velocity $\delta u_l \sim l$ for $l \ll l_\nu$. This is mimicked by prescribing a spatially rough power-law correlation function for the Kazantsev model field. For a certain range of exponents of this power law, it is then possible to show analytically that the Kazantsev field is a dynamo (Rogachevskii & Kleeorin 1997, Vincenzi 2002, Boldyrev & Cattaneo 2004, Celani et al. 2006, Arponen & Horvai 2006). The difficulty lies in establishing a quantitative connection between this result and the real turbulence, in which the decorrelation time of the inertial-range motions is certainly not small but comparable to their turnover time and scale-dependent $\sim l^{2/3}$. It is not known whether setting it to zero changes the dynamo properties of the velocity field enough to render the white-noise model irrelevant. If the white-noise velocity is on some level acceptable, it is not known what choice of its roughness exponent (which determines whether it is a dynamo!) makes it a good model of the inertial-range turbulent velocity field. The authors cited above used a plausible argument (first suggested by Vainshtein 1982), which led them to predict dynamo action. However, this prediction is purely a *quantitative* mathematical outcome of analyzing a synthetic velocity field that is at best a passable *qualitative* representation of real turbulence. In the absence of a physical model of the inertial-range dynamo, the validity of this prediction remains in doubt.

It is natural to ask whether any of the quantitative predictions based on the Kazantsev model are borne out by our numerical results. One such prediction is the scaling (8) of the growth rate, which cannot as yet be verified numerically. Another, due to Rogachevskii & Kleeorin (1997) and to Boldyrev & Cattaneo (2004), is the expectation that the asymptotic dynamo threshold $Rm_c^{(\infty)}$ for $Pm \ll 1$ should be approximately 7 times higher than a similar threshold $Rm_c \sim 60$ for the $Pm \gg 1$ case (see figure 1(b); in the Kazantsev model, the latter threshold is computed by using a velocity field with a smooth spatial correlator, see Novikov et al. 1983). This would imply $Rm_c^{(\infty)} \sim 400$, which is an overestimate by at least a factor of 2 (see section 2.2) — certainly not a damning contradiction, but somewhat short of a confirmation of the theory. Finally, Boldyrev & Cattaneo (2004) predict a (stretched) exponential fall off of the magnetic-field correlation function at $l > l_\eta$, so the magnetic energy is concentrated sharply at the resistive scale. This appears to be at odds with the trend for the magnetic-energy spectrum to develop a negative slope above the resistive scale, reported in section 2.4 (for example, a k^{-1} spectrum would imply that $\delta B_l \sim \text{const}$, i.e., the correlation function is flat rather than falling off exponentially). We reiterate, however, that at resolutions currently available to us, we are unable to claim definitively that the spectral peak is not, in fact, at the resistive scale.

Is there an alternative to the inertial-range dynamo? It might be worth asking whether the randomly forced outer-scale motions could act as a dynamo despite (or in concert with) the turbulence in the inertial range. Indeed, how essential is the

physical difference between the outer-scale motion, whose decorrelation time ($\sim L/U$) is long compared with the inertial-range motions, and a mean flow, whose correlation time is infinite? Can both the mean-flow-driven dynamo found by Ponty et al. (2005) and the fluctuation dynamo reported here by us be manifestations of some universal basic mechanism — for example, of the field amplification by a combined action of a persistent (slowly changing) large-scale (outer-scale) shear and small-scale (inertial-range) turbulent fluctuations (a nonhelical mean-field dynamo of this type has been proposed theoretically by Rogachevskii & Kleeorin 2003)?

An unambiguous signature of this or any other type of outer-scale-driven dynamo would be the convergence of the growth rate to an Rm -independent limit (9). One way to investigate numerically whether there is a smooth connection between the mean-flow dynamo and the randomly forced one would be to construct stability curves $Rm_c(Re)$ for a series of numerical experiments with an inhomogeneous body force (similar to Ponty et al. 2005), which however, is artificially decorrelated with a prescribed correlation time τ_{corr} . The limit $\tau_{\text{corr}} = \infty$ corresponds to the turbulence with a mean flow. As τ_{corr} is reduced, the mean flow should develop a slow time dependence and at $\tau_{\text{corr}} \sim L/U$, the situation would become equivalent to the randomly forced case discussed here.

3. Turbulent Induction

The turbulent magnetic induction is the tangling of a uniform (or large-scale) mean magnetic field by turbulence, which produces magnetic energy at small scales. The mean field may be due to some external imposition or to a mean-field dynamo. Broadly speaking, whatever is the mechanism that generates and/or maintains a magnetic field, the turbulent induction is a nonlocal energy transfer process whereby this field couples to motions at smaller scales to give rise to magnetic fluctuations at those scales. In any real system, it is only a part of a bigger picture of how the magnetic field is generated and shaped. Given a multiscale observed or simulated magnetic field, one does not generally have enough information (or understanding), to tell whether it has originated from the fluctuation dynamo, from the mean-field dynamo plus the turbulent induction or from some combination of the two. However, in the computer, the turbulent-induction effect can be isolated by measuring the response to an imposed uniform field in the subcritical cases, in which the magnetic field would otherwise decay (this approach has been popular in liquid-metal experiments; see, e.g., Odier et al. 1998, Bourgoin et al. 2002, Spence et al. 2006). Table 3 details a number of such runs, done using the same numerical set up as that detailed in section 2.1. We shall see that examining their properties is both instructive in itself and may be revealing about the nature of the fluctuation dynamo.

Mathematically, if the magnetic field is represented as a sum of a uniform mean field and a fluctuating part, $\mathbf{B} = \mathbf{B}_0 + \delta\mathbf{B}$, the fluctuating field satisfies

$$\frac{\partial \delta\mathbf{B}}{\partial t} + \mathbf{u} \cdot \nabla \delta\mathbf{B} = \delta\mathbf{B} \cdot \nabla \mathbf{u} + \eta \nabla^2 \delta\mathbf{B} + \mathbf{B}_0 \cdot \nabla \mathbf{u}. \quad (10)$$

This is simply the induction equation (2) with a source term, which, in the absence

Table 3. Index of runs — Part III (runs with a mean field)

| Run | Res. | B_0 | η | Rm | Pm | Re | Re_λ | u_{rms} | δB_{rms} | Fig. |
|-------------------------------|------------------|-----------|----------------------|------|---------|------|--------------|------------------|-------------------------|---------|
| $\nu_2 = 5 \times 10^{-4}$ | | | | | | | | | | |
| C1-sat | 256 ³ | 0 | 5×10^{-4} | 390 | 1.0 | 390 | 149 | 1.22 | 0.49 | 7(b) |
| B2-sat | 256 ³ | 0 | 10^{-3} | 200 | 0.5 | 410 | 149 | 1.28 | 0.42 | 7(b) |
| m0 | 128 ³ | 1 | 2×10^{-3} | 103 | 0.25 | 410 | 169 | 1.29 | 0.74 | 7(a) |
| m1 | 128 ³ | 10^{-1} | 2×10^{-3} | 98 | 0.25 | 390 | 161 | 1.24 | 0.54 | 7(a) |
| m2 | 128 ³ | 10^{-2} | 2×10^{-3} | 109 | 0.25 | 440 | 118 | 1.37 | 0.136 | 7(a) |
| m3/M1.1 | 128 ³ | 10^{-3} | 2×10^{-3} | 109 | 0.25 | 440 | 111 | 1.37 | 0.021 | 7(a,b) |
| m4 | 128 ³ | 10^{-4} | 2×10^{-3} | 112 | 0.25 | 450 | 114 | 1.41 | 0.0025 | 7(a) |
| m5 | 128 ³ | 10^{-5} | 2×10^{-3} | 112 | 0.25 | 450 | 114 | 1.41 | 0.000165 | 7(a) |
| M1.2 | 128 ³ | 10^{-3} | 4×10^{-3} | 57 | 0.125 | 460 | 113 | 1.43 | 0.0066 | 7(b) |
| M1.3 | 128 ³ | 10^{-3} | 10^{-2} | 23 | 0.05 | 450 | 115 | 1.42 | 0.0030 | 7(b) |
| M1.4 | 128 ³ | 10^{-3} | 2×10^{-2} | 11.6 | 0.025 | 470 | 117 | 1.46 | 0.0020 | 7(b) |
| M1.5 | 128 ³ | 10^{-3} | 4×10^{-2} | 5.5 | 0.0125 | 440 | 110 | 1.39 | 0.00132 | 7(b) |
| M1.6 | 128 ³ | 10^{-3} | 10^{-1} | 2.2 | 0.005 | 440 | 115 | 1.39 | 0.00074 | 7(b) |
| M1.7 | 128 ³ | 10^{-3} | 2×10^{-1} | 1.08 | 0.0025 | 430 | 113 | 1.36 | 0.00037 | 7(b) |
| M1.8 | 128 ³ | 10^{-3} | 4×10^{-1} | 0.54 | 0.00125 | 430 | 112 | 1.35 | 0.00020 | 7(b) |
| M1.9 | 128 ³ | 10^{-3} | 1 | 0.22 | 0.0005 | 440 | 115 | 1.39 | 0.000069 | 7(b) |
| $\nu_2 = 2.5 \times 10^{-4}$ | | | | | | | | | | |
| D1-sat* | 512 ³ | 0 | 2.5×10^{-4} | 710 | 1.0 | 710 | 185 | 1.11 | 0.53 | 7(b) |
| C2-sat* | 256 ³ | 0 | 5×10^{-4} | 380 | 0.5 | 760 | 210 | 1.20 | 0.45 | 7(b) |
| B3-sat | 256 ³ | 0 | 10^{-3} | 210 | 0.25 | 840 | 230 | 1.30 | 0.35 | 7(b) |
| M2.1 | 256 ³ | 10^{-3} | 2×10^{-3} | 105 | 0.125 | 840 | 157 | 1.32 | 0.0088 | 7(b) |
| M2.2 | 256 ³ | 10^{-3} | 4×10^{-3} | 53 | 0.0625 | 840 | 155 | 1.33 | 0.0053 | 7(b) |
| M2.3 | 256 ³ | 10^{-3} | 10^{-2} | 21 | 0.025 | 830 | 156 | 1.31 | 0.0030 | 7(b) |
| $\nu_2 = 1.25 \times 10^{-4}$ | | | | | | | | | | |
| C3-sat* | 256 ³ | 0 | 5×10^{-4} | 380 | 0.25 | 1530 | 350 | 1.20 | 0.47 | 7(b) |
| M3.1 | 256 ³ | 10^{-3} | 10^{-3} | 210 | 0.125 | 1690 | 230 | 1.33 | 0.023 | 7(b) |
| M3.2 | 256 ³ | 10^{-3} | 2×10^{-3} | 111 | 0.0625 | 1770 | 230 | 1.39 | 0.0132 | 7(b) |
| $\nu_8 = 10^{-20}$ | | | | | | | | | | |
| HM1 | 256 ³ | 10^{-3} | 10^{-3} | 230 | 0.062 | 3700 | 340 | 1.45 | 0.027 | 7(b), 8 |
| HM2 | 256 ³ | 10^{-3} | 2×10^{-3} | 114 | 0.031 | 3600 | 330 | 1.43 | 0.0109 | 7(b), 8 |
| HM3 | 256 ³ | 10^{-3} | 4×10^{-3} | 56 | 0.0160 | 3500 | 320 | 1.41 | 0.0071 | 7(b), 8 |
| HM4 | 256 ³ | 10^{-3} | 10^{-2} | 22 | 0.0065 | 3400 | 310 | 1.39 | 0.0034 | 7(b), 8 |
| HM7 | 256 ³ | 10^{-3} | 10^{-1} | 2.3 | 0.00063 | 3600 | 330 | 1.43 | 0.00067 | 7(b), 8 |

of dynamo action, will give rise to a saturated level of the magnetic-fluctuation energy. Equation (10) is linear in $\delta \mathbf{B}$. Therefore, for dynamically weak mean fields, the saturated magnetic energy should be proportional to the mean-field energy:

$$\langle |\delta \mathbf{B}|^2 \rangle = f(Rm) B_0^2. \quad (11)$$

The coefficient of proportionality $f(Rm)$ in this relation is expected to be an increasing function of Rm . At large Rm , this coefficient can be large, $f(Rm) \gg 1$ and the relation

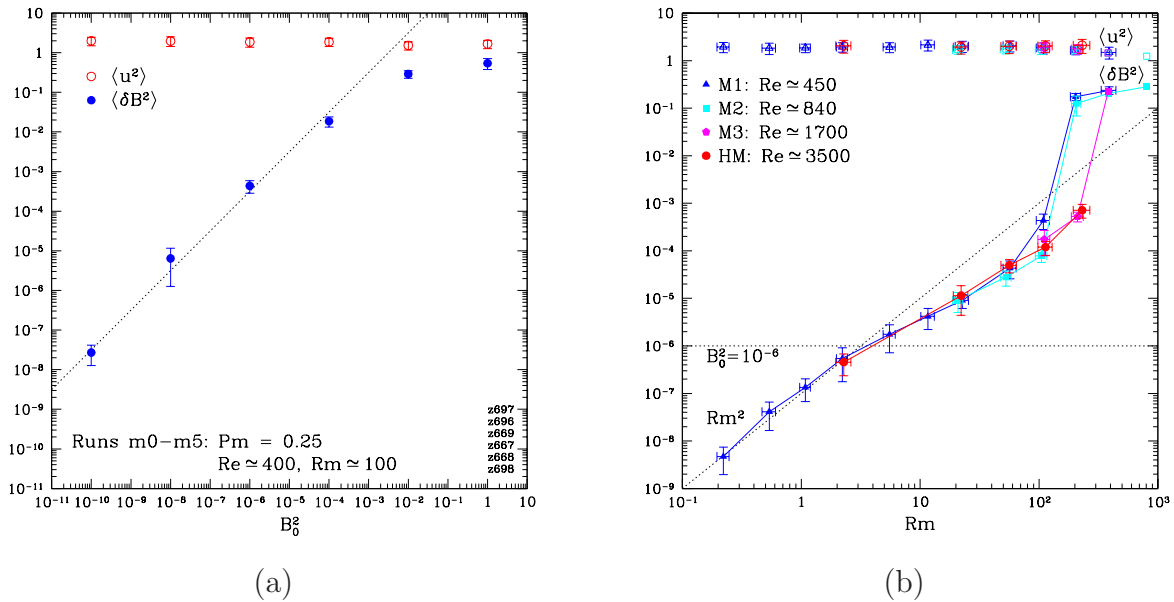


Figure 7. (a) The mean square induced field $\langle |\delta \mathbf{B}|^2 \rangle$ vs. the mean field squared B_0^2 in the subcritical regime (no dynamo). These runs correspond to the decaying run A3 (table 1) with an imposed mean field. Error bars show the mean square deviation from the average value in the set of snapshots over which the time average was done. The dotted line shows the slope corresponding to a linear dependence. (b) The mean square induced field $\langle |\delta \mathbf{B}|^2 \rangle$ vs. Rm for runs with $B_0 = 10^{-3}$ in the subcritical regime, $Rm < Rm_c$. For $Rm > Rm_c$, the saturated energies for $B_0 = 0$ runs are shown (the saturated states of runs B2, B3, C1, C2, C3 are denoted B2-sat, etc. in table 3). The reference slope corresponding to Rm^2 is shown for comparison with the quasistatic theory (section 3.1).

(11) will hold only as long as not only the mean field but also the fluctuating field is dynamically weak, $\langle |\delta \mathbf{B}|^2 \rangle \ll \langle |\mathbf{u}|^2 \rangle$. If it is not, the back reaction will take over as the controlling agent in the saturation mechanism, resulting in a dynamical state with $\langle |\delta \mathbf{B}|^2 \rangle \sim \langle |\mathbf{u}|^2 \rangle$. This simple picture is, unsurprisingly, borne out by the numerical experiment: figure 7(a) illustrates this point.

3.1. Turbulent Induction at Low Rm

It is rather straightforward to make a theoretical prediction about the form of $f(Rm)$ in the limit of small Rm . The diffusion term in (10) dominates the nonlinear terms and the saturated state is governed by the “quasistatic” balance

$$\eta \nabla^2 \delta \mathbf{B} = -\mathbf{B}_0 \cdot \nabla \mathbf{u}, \quad (12)$$

which immediately implies $\langle |\delta \mathbf{B}|^2 \rangle \sim Rm^2 B_0^2$.

In the wave-number space, the quasistatic approximation (12) returns an explicit form of the angle-integrated, one-dimensional magnetic-energy spectrum $M(k)$ in terms

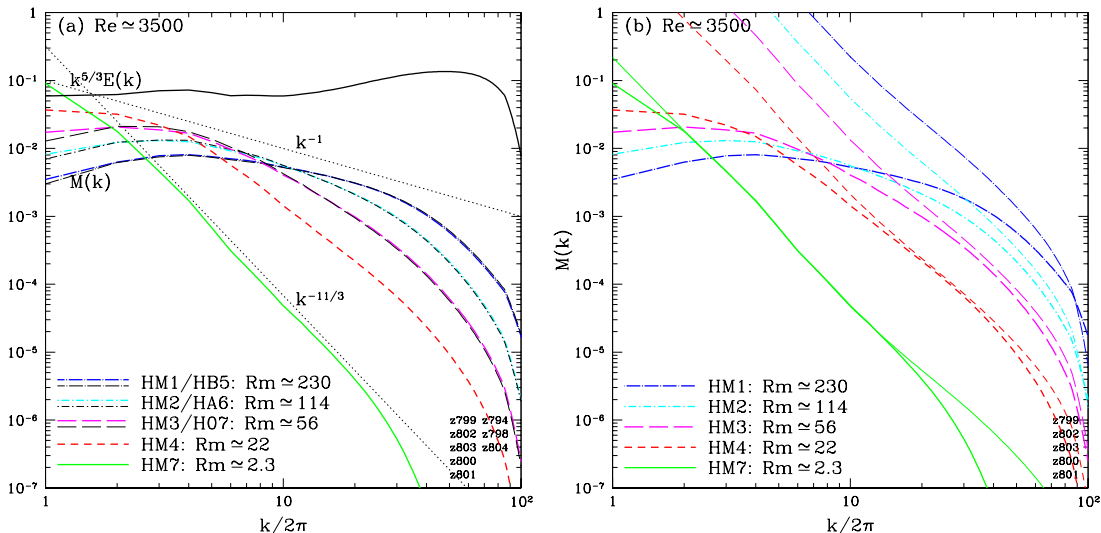


Figure 8. (a) The magnetic-energy spectra, normalized by $\langle |\delta \mathbf{B}|^2 \rangle / 2$ and time-averaged, for the runs with the 8th-order hyperviscosity (effective $Re \sim 3500$) and $B_0 = 10^{-3}$ (series HM). For comparison, normalized magnetic-energy spectra for the analogous decaying runs with $B_0 = 0$ are shown. The decaying spectra (runs HB5, HA6, H07) coincide with the steady-state spectra of induced fluctuations (runs HM1, HM2, HM3) almost exactly. The slopes corresponding to the Golitsyn (1960) $k^{-11/3}$ and Ruzmaikin & Shukurov (1982) k^{-1} spectra are given for reference. The kinetic-energy spectrum, normalized by $\langle |\mathbf{u}|^2 \rangle / 2$, time-averaged and compensated by $k^{5/3}$, is also plotted (it is the same for all runs). (b) The same spectra as in (a) for the HM series (bold lines) compared with the linear quasistatic-theory prediction (13) (thin lines). For all runs except HM7, B_0 in (13) has been replaced with $\langle |\mathbf{B}|^2 \rangle^{1/2}$.

of the kinetic-energy spectrum $E(k)$:

$$\eta k^2 \delta \mathbf{B}_{\mathbf{k}} = i(\mathbf{k} \cdot \mathbf{B}_0) \mathbf{u}_{\mathbf{k}} \quad \Rightarrow \quad M(k) = \frac{B_0^2}{3\eta^2} \frac{E(k)}{k^2}. \quad (13)$$

If the kinetic energy spectrum is Kolmogorov, one obtains $M(k) \sim B_0^2 \eta^{-2} \varepsilon^{2/3} k^{-11/3}$ (Golitsyn 1960). Note that we limit ourselves to the case of weak magnetic field (for some numerical experiments with a dynamically strong field, see, e.g., Zikanov & Thess 1998, Knaepen et al. 2004, and references therein).

The predictions of the quasistatic theory are rigorous and, of course, confirmed by the numerical simulations. Figure 7(b) shows that the Rm^2 scaling of the induced magnetic energy holds, under our definition of Rm , up to $Rm \sim 2$, which is also approximately the point at which $\langle |\delta \mathbf{B}|^2 \rangle$ becomes larger than B_0^2 . The Golitsyn (1960) spectrum is also there — as shown in figure 8(a) for the run HM7. While this spectrum is solidly established in the laboratory (e.g., Odier et al. 1998, Bourgoin et al. 2002) and was successfully simulated by Ponty et al. (2004) using LES, our result appears to be the first time that it has been obtained in a direct numerical simulation of the low- Rm MHD turbulence. Although no element of surprise was present here, we consider it reassuring to have dotted this particular i.

3.2. Turbulent Induction at High Rm

As Rm increases, the quasistatic approximation (12) ceases to be valid, the nonlinear terms in (10) are no longer negligible and the dependence $f(Rm)$ becomes nontrivial. Figure 7(b) shows how at $Rm > 2$ it flattens until, around $Rm \sim 200$, the fluctuation dynamo sets in, overwhelms the turbulent induction and brings the magnetic energy into a saturated state determined not by Rm but by the nonlinear back reaction ($\langle |\delta \mathbf{B}|^2 \rangle \sim \langle |\mathbf{u}|^2 \rangle$).⁴ The close agreement between the magnetic energies for the Laplacian and hyperviscous runs with different Re suggests that these results are converged in Re .

While one might dwell on the question of what the asymptotic form of $f(Rm)$ for large Rm should be (e.g., Moffatt 1961, Parker 1969, Saffman 1964, Low 1972, Vainshtein & Cattaneo 1992, Cattaneo et al. 1995), it is perhaps reasonable to ask first whether, in view of our claim that the fluctuation dynamo is unavoidable at sufficiently large Rm , the problem is meaningfully posed. The short answer is, obviously, no. However, there is a useful way, already intimated at the beginning of section 3, in which the turbulent induction problem can be posed at high Rm .

Firstly, if \mathbf{B}_0 is interpreted as the dynamo-generated field at the resistive scale and above, we may inquire into the behaviour of the magnetic fluctuations below the resistive scale, $l \ll l_\eta$. Since the inertial-range motions at these scales have a shorter correlation time than at $l \sim l_\eta$, we can, indeed, treat this as a problem with a constant mean field and use (10). The quasistatic theory is still valid because the diffusion term is dominant. Thus, the Golitsyn (1960) spectrum is now recovered as the subresistive tail of the magnetic-energy spectrum (Moffatt 1961). In numerical simulations, this is hard to check at current resolutions, but we can compare the magnetic spectra in our simulations with the quasistatic prediction (13) using the full numerically obtained form of $E(k)$ and replacing $B_0 \rightarrow \langle |\mathbf{B}|^2 \rangle^{1/2}$. There is, indeed, a fit below some sufficiently small (resistive) scale, which predictably decreases with increasing Rm .

Secondly, if the dynamo amplifies the magnetic field at the outer scale or above (this is now our mean field \mathbf{B}_0), one might ask how much magnetic energy this will generate via the turbulent induction in the part of the inertial range that lies above the resistive scale, $L \gg l \gg l_\eta$. In (10), the diffusive term can now be ignored. It seems then to be a plausible argument that, if the nonlocal energy transfer from the outer-scale field is important at all, its effect on the inertial-range magnetic fluctuations can be found by balancing the ‘‘source’’ term containing \mathbf{B}_0 with the nonlinear terms, which represent the local interactions between \mathbf{u} and $\delta \mathbf{B}$. This gives (Ruzmaikin & Shukurov 1982)

$$\delta B_l \sim B_0 \quad \Rightarrow \quad M(k) \sim B_0^2 k^{-1}. \quad (14)$$

The same spectrum and the consequent scaling $\langle |\delta \mathbf{B}|^2 \rangle \sim (\ln Rm) B_0^2$ were obtained

⁴Note that while the scaling of $\langle |\delta \mathbf{B}|^2 \rangle$ with $Rm - Rm_c$ just above the transition to dynamo is an interesting theoretical question (P  tr  lis & Fauve 2001), determining this scaling numerically is not currently possible because of the extreme long-time fluctuations close to criticality and the consequent need for unaffordably long runs.

in several closure calculations assuming a weak mean field and no dynamo (Kleeorin et al. 1990, Kleeorin & Rogachevskii 1994, Kleeorin et al. 1996) (see, however, an argument by Moffatt (1961), based on the mathematical analogy between the magnetic field and vorticity and leading to a $k^{1/3}$ spectrum). Note that all this only applies in the limit $\langle |\delta \mathbf{B}|^2 \rangle \ll \langle |\mathbf{u}|^2 \rangle$ (which is where our simulations are; see figure 7(b)). Otherwise, dynamical effects, such as the Alfvénization of the turbulence, will be important and determine the shape of the saturated state.

The scaling (14) can only be realized if an outer-scale magnetic field really exists and if the tangling of this field by turbulence is not superceded by an inertial-range dynamo, as discussed in section 2.6. Thus, it is only a possibility and, indeed, a signature property, if the fluctuation dynamo found by us is, in fact, an outer-scale dynamo. As we explained in section 2.4, our numerical simulations are not sufficiently asymptotic to determine the spectrum of magnetic fluctuations. The apparent tendency towards a negative spectral slope reported in section 2.4 may be a telling sign in view of the theoretical result (14). We have plotted the reference k^{-1} slopes in figure 3 and figure 6(e,f). We leave it to the reader’s judgement to decide if this scaling might, indeed, be emerging there.

An important observation must be made in this context. The saturated magnetic-energy spectra in the subcritical runs with an imposed weak mean field turn out, after normalization, to be *exactly* the same as the normalized spectra of the corresponding decaying runs without the mean field (see figure 8(a)). Furthermore, as reported in section 2.4, no qualitative change occurs in the magnetic-energy spectrum as the dynamo threshold is crossed. This seems to tell us that the same mechanism is responsible for setting the shape of the spectrum of the magnetic fluctuations induced by a mean field and of the decaying or growing such fluctuations in the absence of a mean field.

4. Conclusions

Let us reiterate the main numerical results and theoretical points presented above.

- Fluctuation dynamo exists in nonhelical randomly forced homogeneous turbulence of a conducting fluid with low magnetic Prandtl number (section 2.2). The critical magnetic Reynolds number for this dynamo is at most three times larger than for $Pm \geq 1$: defined by (4), it is $Rm_c \lesssim 200$ for $Re \gtrsim 6000$, although there is a larger peak value at a somewhat smaller Re .
- The nature of the dynamo and its stability curve $Rm_c(Re)$ are different from the dynamo obtained in simulations and liquid-metal experiments with a mean flow (section 2.5).
- The physical mechanism that enables the sustained growth of magnetic fluctuations in the low- Pm regime is unknown. It is not as yet possible to determine numerically whether the fluctuation dynamo is driven by the inertial-range motions at the resistive scale and consequently has a growth rate $\propto Rm^{1/2}$ in the limit $Rm \rightarrow \infty$,

or rather a constant growth rate comparable to the turnover rate of the outer-scale motions (section 2.6).

- The magnetic-energy spectra in the low- Pm regime are qualitatively different from the $Pm \geq 1$ case and appear to develop a negative spectral slope, which may be consistent with k^{-1} , but cannot be definitively resolved (section 2.4). The spectra of the growing field are similar to those for the decaying field at lower Rm and to the saturated spectra of the induced magnetic energy in the presence of a weak mean field (section 3.2).
- At very low Rm , the magnetic fluctuations induced via the tangling by turbulence of a weak mean field are well described by the quasistatic approximation. The $k^{-11/3}$ spectrum is confirmed (section 3.1).

While these results leave a frustrating number of questions unanswered and do not entirely clear up the confusion over the exact nature of the low- Pm dynamo, they do at least confirm that the object of this confusion exists. It is important to check in independent numerical experiments both that our conclusions hold and whether the value of the dynamo threshold obtained by us is universal. Some promising numerical experiments aimed at elucidating the nature of the dynamo and the role of the mean flow are proposed in section 2.5 and section 2.6.

The main conclusion of this work is the confirmation that nature will always find a way to make magnetic field where turbulence of a conducting fluid is present. In the astrophysical context, the low- Pm fluctuation dynamo is particularly (although by no means solely) important in the context of solar magnetism. While there is ample observational evidence that small-scale magnetic fluctuations pervade the solar photosphere (e.g., Domínguez Cerdeña et al. 2003, Socas-Navarro & Lites 2004, Trujillo Bueno et al. 2004, Solanki et al. 2006), the numerical evidence used to argue that the turbulent fluctuation dynamo is responsible has thus far been based on numerical simulations with $Pm \geq 1$ (Cattaneo 1999, Cattaneo et al. 2003, Bushby 2007). The existence of the low- Pm fluctuation dynamo that we have established for an idealized homogeneous MHD turbulence gives us confidence that attempts to demonstrate self-consistent magnetic-field amplification in more realistic simulations of solar convection with $Pm \ll 1$ will eventually prove successful.

Acknowledgments

We thank A. Brandenburg, B. Dubrulle, S. Fauve, C. Forest, N. Haugen, D. Hughes, N. Kleeorin, P. Mininni, J. Papaloizou, J.-F. Pinton, F. Plunian, Y. Ponty, F. Rincon, I. Rogachevskii, A. Shukurov and N. Weiss for valuable discussions at various stages of this project. We are grateful to V. Decyk (UCLA) who has kindly provided his FFT libraries from the UPIC framework. A.A.S. was supported by a PPARC Advanced Fellowship. He also thanks the USDOE Center for Multiscale Plasma Dynamic for travel support and the UCLA Plasma Group for its hospitality. A.B.I. was supported by the USDOE

Center for Multiscale Plasma Dynamics. T.A.Y. was supported by a UKAFF Fellowship and the Newton Trust. Simulations were done on UKAFF (Leicester), NCSA (Illinois) and the Dawson cluster (UCLA Plasma Group).

References

- Arponen H & Horvai P 2006 *Preprint nlin.CD/0610023*.
- Batchelor G K 1950 *Proc. R. Soc. London A* **201**, 405.
- Bayliss R A, Forest C B, Nornberg M D, Spence E J & Terry P W 2007 *Phys. Rev. E* **75**, 026303.
- Berhanu M, Monchaux R, Fauve S, Mordant N, Pétrélis F, Chiffaudel A, Daviaud F, Dubrulle B, Marié L, Ravelet F, Bourgoïn M, Odier P, Pinton J F & Volk R 2007 *Europhys. Lett.* **77**, 59001.
- Boldyrev S & Cattaneo F 2004 *Phys. Rev. Lett.* **92**, 144501.
- Bourgoïn M, Marié L, Pétrélis F, Gasquet C, Guigon A, Luciani J B, Moulin M, Namer F, Burguete J, Chiffaudel A, Daviaud F, Fauve S, Odier P & Pinton J F 2002 *Phys. Fluids* **14**, 3046.
- Brandenburg A 2001 *Astrophys. J.* **550**, 824.
- Brandenburg A, Jennings R L, Nordlund Å, Rieutord M, Stein R F & Tuominen I 1996 *J. Fluid Mech.* **306**, 325.
- Brandenburg A & Subramanian K 2005 *Phys. Rep.* **417**, 1.
- Bushby P 2007 private communication.
- Cattaneo F 1999 *Astrophys. J.* **515**, L39.
- Cattaneo F, Emonet T & Weiss N 2003 *Astrophys. J.* **588**, 1183.
- Cattaneo F, Kim E J, Proctor M & Tao L 1995 *Phys. Rev. Lett.* **75**, 1522.
- Celani A, Mazzino A & Vincenzi D 2006 *Proc. R. Soc. London A* **462**, 137.
- Chertkov M, Falkovich G, Kolokolov I & Vergassola M 1999 *Phys. Rev. Lett.* **83**, 4065.
- Childress S & Gilbert A 1995 *Stretch, Twist, Fold: The Fast Dynamo* Springer Berlin.
- Christensen U, Olson P & Glatzmaier G A 1999 *Geophys. J. Int.* **138**, 393.
- Domínguez Cerdeña I, Sánchez Almeida J & Kneer F 2003 *Astron. Astrophys.* **407**, 741.
- Galanti B, Sulem P L & Pouquet A 1992 *Geophys. Astrophys. Fluid Dyn.* **66**, 183.
- Galloway D J & Proctor M R E 1992 *Nature (London)* **356**, 691.
- Golitsyn G S 1960 *Sov. Phys. Doklady* **5**, 536.
- Haugen N E L, Brandenburg A & Dobler W 2004 *Phys. Rev. E* **70**, 016308.
- Iskakov A B, Schekochihin A A, Cowley S C, McWilliams J C & Proctor M R E 2007 *Preprint astro-ph/0702291*.
- Kazantsev A P 1968 *Sov. Phys. JETP* **26**, 1031.
- Kleorin N, Mond M & Rogachevskii I 1996 *Astron. Astrophys.* **307**, 293.
- Kleorin N & Rogachevskii I 1994 *Phys. Rev. E* **50**, 2716.
- Kleorin N, Rogachevskii I & Ruzmaikin A 1990 *Sov. Phys. JETP* **70**, 878.
- Knaepen B, Kassinos S & Carati D 2004 *J. Fluid Mech.* **513**, 199.
- Kulsrud R M & Anderson S W 1992 *Astrophys. J.* **396**, 606.
- Laval J P, Blaineau P, Leprovost N, Dubrulle B & Daviaud F 2006 *Phys. Rev. Lett.* **96**, 204503.
- Léorat J, Pouquet A & Frisch U 1981 *J. Fluid Mech.* **104**, 419.
- Low B C 1972 *Astrophys. J.* **173**, 549.
- Meneguzzi M, Frisch U & Pouquet A 1981 *Phys. Rev. Lett.* **47**, 1060.
- Mininni P, Alexakis A & Pouquet A 2005 *Phys. Rev. E* **72**, 046302.
- Mininni P D 2006 *Phys. Plasmas* **13**, 056502.
- Mininni P D 2007 *Preprint physics/0702109*.
- Mininni P D & Montgomery D C 2005 *Phys. Rev. E* **72**, 056320.
- Mininni P, Ponty Y, Montgomery D C, Pinton J F, Politano H & Pouquet A 2005 *Astrophys. J.* **626**, 853.

- Moffatt H K 1978 *Magnetic Field Generation in Electrically Conducting Fluids* Cambridge University Press Cambridge.
- Moffatt H K & Saffman P G 1963 *Phys. Fluids* **7**, 155.
- Moffatt K 1961 *J. Fluid Mech.* **11**, 625.
- Monchaux R, Berhanu M, Bourgoin M, Moulin M, Odier P, Pinton J F, Volk R, Fauve S, Mordant N, Pétrélis F, Chiffaudel A, Daviaud F, Dubrulle B, Gasquet C, Marié L & Ravelet F 2007 *Phys. Rev. Lett.* **98**, 044502.
- Nordlund Å, Brandenburg A, Jennings R L, Rieutord M, Ruokolainen J, Stein R F & Tuominen I 1992 *Astrophys. J.* **392**, 647.
- Nore C, Brachet M E, Politano H & Pouquet A 1997 *Phys. Plasmas* **4**, 1.
- Novikov V G, Ruzmaikin A A & Sokoloff D D 1983 *Sov. Phys. JETP* **58**, 527.
- Odier P, Pinton J F & Fauve S 1998 *Phys. Rev. E* **58**, 7397.
- Ossendrijver M 2003 *Astron. Astrophys. Rev.* **11**, 287.
- Ott E 1998 *Phys. Plasmas* **5**, 1636.
- Parker E N 1969 *Astrophys. J.* **138**, 226.
- Peffley N L, Cawthorne A B & Lathrop D P 2000 *Phys. Rev. E* **61**, 5287.
- Pétrélis F & Fauve S 2001 *Eur. Phys. J. B* **22**, 273.
- Pétrélis F & Fauve S 2006 *Europhys. Lett.* **76**, 602.
- Ponty Y, Mininni P D, Montgomery D C, Pinton J F, Politano H & Pouquet A 2005 *Phys. Rev. Lett.* **94**, 164502.
- Ponty Y, Mininni P D, Pinton J F, Politano H & Pouquet A 2006 *Preprint physics/0601105*.
- Ponty Y, Politano H & Pinton J F 2004 *Phys. Rev. Lett.* **92**, 144503.
- Ravelet F, Chiffaudel A, Daviaud F & Léorat J 2005 *Phys. Fluids* **17**, 117104.
- Roberts P H & Glatzmaier G A 2000 *Rev. Mod. Phys.* **72**, 1081.
- Rogachevskii I & Kleeorin N 1997 *Phys. Rev. E* **56**, 417.
- Rogachevskii I & Kleeorin N 2003 *Phys. Rev. E* **68**, 036301.
- Ruzmaikin A A & Shukurov A M 1982 *Astrophys. Space Sci.* **82**, 397.
- Saffman P G 1964 *J. Fluid Mech.* **18**, 449.
- Schekochihin A A, Cowley S C, Maron J L & McWilliams J C 2004 *Phys. Rev. Lett.* **92**, 054502.
- Schekochihin A A, Cowley S C, Taylor S F, Maron J L & McWilliams J C 2004 *Astrophys. J.* **612**, 276.
- Schekochihin A A, Haugen N E L, Brandenburg A, Cowley S C, Maron J L & McWilliams J C 2005 *Astrophys. J.* **625**, L115.
- Socas-Navarro H & Lites B W 2004 *Astrophys. J.* **616**, 587.
- Solanki S K, Inhester B & Schüssler M 2006 *Rep. Prog. Phys.* **69**, 563.
- Spence E J, Nornberg M D, Jacobson C M, Kendrick R D & Forest C B 2006 *Phys. Rev. Lett.* **96**, 055002.
- Stepanov R & Plunian F 2007 *J. Turbulence* **7**, 39.
- Trujillo Bueno J, Shchukina N G & Asensio Ramos A 2004 *Nature (London)* **430**, 326.
- Vainshtein S I 1982 *Magnetohydrodynamics* **28**, 123.
- Vainshtein S I & Cattaneo F 1992 *Astrophys. J.* **393**, 165.
- Vincenzi D 2002 *J. Stat. Phys.* **106**, 1073.
- Widrow L M 2002 *Rev. Mod. Phys.* **74**, 775.
- Wilkin S L, Barengi C F & Shukurov A 2007 *Preprint astro-ph/0702261*.
- Zeldovich Y B, Ruzmaikin A A, Molchanov S A & Sokoloff D D 1984 *J. Fluid Mech.* **144**, 1.
- Zikanov O & Thess A 1998 *J. Fluid Mech.* **358**, 299.